Solid State Science and Technology, Vol. 33, No. 2 (2025) 87-96
https://doi.org/10.66514/ssst-33-2-87-96

First-Principles Investigation on Structural Distortion and Electronic Tuning in La-Doped MgB_2 Superconductors

Siti Fatimah Saipuddin[1,2,*], Azhan Hashim[3], Nurbaisyatul Ermiza Suhaimi[1], Rabiatul Adawiyyah Rosli[1], Nur Hamizah Mohd Zaki[1,2], Fatin Nabilah Sazman[1,2] Siti Aisyah Yasup[1]

[1]*Faculty of Applied Sciences, Universiti Teknologi MARA (UiTM) 40450 Shah Alam, Selangor, Malaysia*
[2]*Ionic Materials and Devices (iMADE) Research Laboratory, Institute of Sciences (IOS), Universiti Teknologi MARA (UiTM), 40450 Shah Alam, Selangor, Malaysia*
[3]*Faculty of Applied Sciences, Universiti Teknologi MARA (UiTM) Pahang, Jengka Campus, 26400 Bandar Tun Abdul Razak, Pahang, Malaysia*

**Corresponding author (email: sitifatimah7020@uitm.edu.my)*

(Received: 1 December 2025 / Revised: 18 December 2025 / Accepted: 22 December 2025 / Published online: 23 December 2025)

ABSTRACT

Rare-earth doping is a promising strategy for enhancing the superconducting performance of magnesium diboride (MgB_2) superconductor by modifying its lattice structure and electronic band characteristics. In this study, first-principles Density Functional Theory (DFT) calculations were carried out using the CASTEP module to evaluate the structural and electronic effects of lanthanum (La) substitution at the magnesium site of MgB_2. A 2×2×2 supercell was constructed, and doping concentrations of 25%, 50%, and 75% were simulated. Geometry optimization, bond length measurement, electronic band structure, and density of states (DOS) analyses were performed using the GGA-PBESOL functional with validated convergence parameters. Results indicate that La doping introduces significant lattice expansion and La–B bond elongation, causing structural distortion due to its large ionic radius.

Keywords: CASTEP; Density Functional Theory; MgB_2, rare-earth doping; superconductivity

INTRODUCTION

Superconductivity is a phenomenon in which materials exhibit zero electrical resistance and expel magnetic flux when cooled below a critical temperature (T_c). Since its discovery in mercury by Heike Kamerlingh Onnes in 1911, the field has progressed toward compounds with higher T_c values [1-3]. A significant discovery of 39 K superconductivity in magnesium diboride (MgB_2) marking the highest T_c among conventional phonon-

mediated superconductors [4]. MgB_2 is unique for its two-gap superconductivity arising from σ- and π-bonding electrons, with the σ band dominating the mechanism and challenging conventional BCS assumptions [5]. Its simple structure and low-cost synthesis make it attractive for superconducting magnets, power cables, and levitation technologies.

However, its technological use is limited by low critical current density (J_c) under magnetic fields. Methods such as chemical doping, ion irradiation, and nano-structuring have been used to enhance flux pinning [6]. Chemical doping is particularly effective when the structural coherence of MgB_2 is maintained [7-8]. Among various dopants, rare-earth elements are of interest due to their strong electron-donating character and ability to modify the electronic structure without severely disrupting the AlB_2-type lattice. Lanthanum (La) is a non-magnetic rare-earth element with partially filled 5*d* states and low electronegativity, making it an effective electron donor for tuning the density of states (DOS) near the Fermi level, which is crucial for superconductivity in MgB_2 [9–11]. La doping has been reported to increase the density of states (DOS) near the Fermi level, improving the critical field and J_c, and reducing anisotropy to enhance grain connectivity [12-13]. First-principles density functional theory (DFT) studies further indicate that La incorporation introduces additional electronic states, induces a slight Fermi-level shift, and preserves the metallic nature of MgB_2 without introducing magnetic pair-breaking effects [10].

This study aims to provide a fundamental understanding of the doping mechanism by quantifying the structural distortions and electronic tuning, specifically near the Fermi level, caused by La incorporation at different levels, thereby clarifying its role in improving the superconducting behaviour of MgB_2.

MATERIALS AND METHODS

Throughout this study, calculations were performed using the CASTEP module within the Materials Studio 2016 package, based on Density Functional Theory (DFT) [14]. The construction of a pristine MgB_2 structure using crystallographic data corresponding to the P6/mmm space group, and the hexagonal unit cell was expanded into a 2×2×2 supercell to accommodate substitutional dopants. The lattice parameters from the Rietveld refined x-ray diffraction pattern from the referred experimental work on pure MgB_2 applying the solid-state reaction method ($a = b = 3.085$ Å, $c = 3.523$ Å; $a=b\neq c$) [15] were applied in the software. Prior to introducing dopants, the pure MgB_2 system underwent structural optimization using three exchange–correlation functionals: LDA-CAPZ [16], GGA-PBE [17], and GGA-PBESOL [18]. The optimized lattice parameters were compared with experimental values and previously reported computational studies [19-20], and percentage deviations were assessed. Based on the closest agreement with reference data, GGA-PBESOL was selected for all subsequent simulations. Convergence tests were then performed to determine the optimal *k*-point sampling and plane-wave cut-off energy, ensuring numerical stability, accuracy, and computational efficiency. These convergence parameters were fixed throughout the study. Figure 1 shows the optimized 2×2×2 supercell of pure MgB_2 crystal structure.

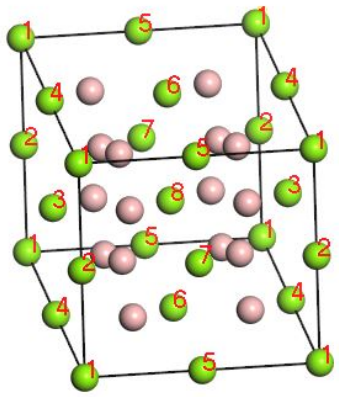

Figure 1. Optimized 2×2×2 supercell of pure MgB_2 crystal structure constructed using Material Studio software. Color coding of Green represents Mg, while red represents boron atoms

Doping was introduced by substituting Mg atoms in the 2×2×2 supercell, which contains eight (8) Mg atoms with La. Substitution of 2, 4, and 6 Mg atoms yielded doping concentrations of 25%, 50%, and 75%, respectively, and each configuration was treated as an independent model [21]. Complete structural relaxation was carried out for every doped system to minimise the total energy and eliminate residual stresses, ensuring that each model reached equilibrium prior to further analysis [22]. Following geometry optimization, electronic structure calculations including band structure and DOS analyses were performed to evaluate the changes in the electronic properties, particularly near the Fermi level, which is most relevant to superconducting behaviour [23]. The structural distortion and electronic tuning upon the introduction of La into the pure crystal structure were investigated.

The structural characteristics of the La-doped MgB_2 systems were analyzed to describe the influence of La substitution on the lattice parameters. The study incorporated the evaluation of bond-length variations around the dopant sites as well as changes in lattice parameters across different doping concentrations. Such structural observations provide critical insight into the atomic-scale distortions induced by substitutional doping.

Complementing the structural calculation, the electronic properties of both pure and La-doped MgB_2 supercells were investigated. The electronic analysis focused on band structure and band gap characteristics, as well as full and partial DOS distributions to determine the extent to which La incorporation alters the electronic behavior of MgB_2, with particular emphasis on features relevant to superconductivity. Simulations were conducted for La doping levels of 25%, 50%, and 75%, enabling systematic comparison with the undoped system and providing a detailed understanding of the progressive electronic modifications arising from increasing dopant concentrations.

RESULTS AND DISCUSSION

The obtained lattice parameters of MgB_2 from the simulations compared to the reported data are presented in Table 1. Among the three functionals examined, the GGA-PBESOL

produced the least difference overall compared to the reference values for the lattice parameter. Thus, GGA-PBESOL was selected for structural optimization and electronic structure calculations throughout this study.

Table 1. Lattice parameters of MgB_2 from the simulations compared to the referred data

Exchange-correlation functionals	Lattice Parameter					
	a / Å	Percent difference (%)	*b* / Å	Percent difference (%)	*c* / Å	Percent difference (%)
Ref. [15]	3.0853		3.083		3.521	
LDA-CAPZ	3.042	- 1.403	3.042	- 1.403	3.500	- 0.596
GGA-PBE	3.084	- 0.042	3.084	- 0.042	3.570	+ 1.392
GGA-PBESOL	3.081	- 0.139	3.081	- 0.139	3.548	+ 0.767

Geometrical optimization was performed on the MgB_2 2×2×2 supercell using the selected GGA-PBESOL exchange–correlation functional. The supercell was derived from the standard hexagonal unit cell. The optimised lattice parameters obtained were *a* = 6.1778 Å, *b* = 6.1786 Å, and *c* = 7.0424 Å. This optimised structure served as the baseline reference for bond length distortion due to doping. Table 2 shows the lattice parameters and bond length measurement between La dopants with neighbouring B atoms.

As shown in Table 2, the introduction of La-dopants induces measurable structural distortions in the MgB_2 supercell. Increasing the concentration of La modifies the lattice constants and perturbs the local bonding environment within the layered structure. The observed expansion of the *a*, *b*, and *c* lattice parameters correlates with the larger ionic radius of La^{3+} (1.03 Å, coordination number = 6) relative to Mg^{2+} (0.72 Å, coordination number = 6), leading to an overall enlargement of the crystal framework. This size mismatch is expected to induce local lattice distortions that can act as effective flux-pinning centers while simultaneously modifying the electronic structure near the Fermi level. This distortion is further supported by the systematic increase in bond lengths between the La dopant and its nearest neighbour B atoms, indicating localised lattice expansion and strain around the substitution sites. Collectively, these structural changes confirm that La doping disrupts the ideal geometry of the pure MgB_2 supercell and introduces significant atomic-level distortions.

Table 2. Lattice parameters of pure 2×2×2 supercell MgB_2 and Bond Length between La-B atoms within crystal structure compared to La-doped crystal structures

Structure	La-conc.(%)	Lattice Parameters (Å)	La-B Bond Length (Å)
Pure 2×2×2 supercell MgB_2	0	a = 6.1778, b = 6.1786, c = 7.040	Mg–B = 2.505, B–B = 1.782 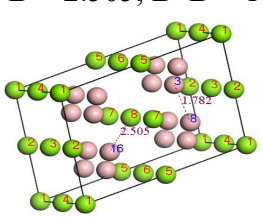
La-doped in 2×2×2 supercell MgB_2	25	a = 6.344, b = 6.344, c = 7.669	La1–B15 = 2.704, La2–B16 = 2.705 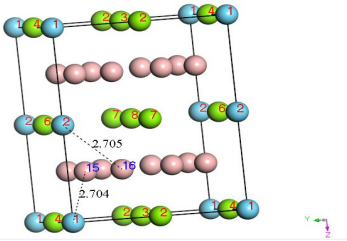
	50	a = 7.017, b = 6.353, c = 7.608	La1–B15 = 2.920, La2–B16 = 2.882 La3–B1 = 2.925, La4–B5 = 2.961 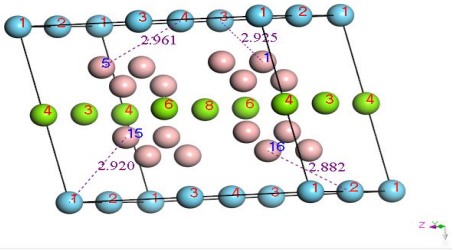
	75	a = 6.651, b = 6.650, c = 8.337	La1–B8 = 2.859, La2–B4 = 2.833 La3–B3 = 2.860, La4–B2 = 2.860 La5–B13 = 2.832, La6–B5 = 2.833 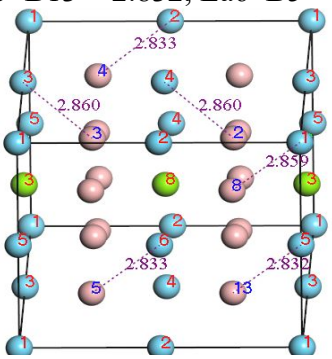

Previous experimental investigations shows that La doping in MgB_2 induces subtle but measurable changes in the lattice parameters, primarily manifested as a slight expansion of the in-plane *a*-axis with increasing La content, while the *c*-axis remains relatively unchanged [13]. This anisotropic lattice response is attributed to the significant ionic radius mismatch between La^{3+} and Mg^{2+}, which introduces local lattice strain without collapsing the hexagonal AlB_2-type structure. Such lattice distortion suggests that La does not fully substitute Mg sites but instead induces local structural perturbations or secondary phase formation, consistent with the preservation of superconductivity accompanied by enhanced flux pinning and hence lead to a modest reduction in the critical temperature.

For electronic properties, the band structures of all configurations were computed to assess the impact of La substitution. Band gap characteristics were obtained by identifying the relative positions of the valence band maximum (VBM) and conduction band minimum (CBM) across the sampled *k*-points. The band gap values for pure and La-doped crystal structures are summarised in Table 3. The results indicate that at 50% La doping, the band gap narrows to 0.48 eV, a significant reduction from the 1.06 eV gap of the pure structure.

From an electronic perspective, the band structure is preserved, maintaining the σ- and π-band features crucial for two-gap superconductivity, while additional electronic states introduced by La near the Fermi level slightly shift the Fermi energy. The resulting increase in the DOS at the Fermi level enhances charge carrier availability and contributes to improved J_C by enhancing the flux pinning without significant suppression of superconductivity [13].

The electronic analysis and the observed lattice expansion that shows local structural distortions, provide a comprehensive understanding of La doping contribution in the modification of both the structural and electronic properties of MgB_2.

The partial DOS analysis reveals distinct changes in the electronic characteristics of MgB_2 upon La doping, as shown in Table 4. In the undoped supercell, a strong Mg 2*p* peak appears near –43 eV (~45 electrons/eV), while states near the Fermi level (0 eV) are dominated by B 2*p* orbitals between –10 and –15 eV, with moderate DOS values (~0.5–1 electron/eV). Although the total DOS at the Fermi level is relatively low, the presence of B 2*p* states reflects the partially metallic character of MgB_2, where σ-bonding within the B layers support its high superconducting transition temperature [9].

La substitution significantly modifies the electronic behaviour. At 25% doping, Mg 2*p* states dominate at –42 eV with 100 electrons/eV, and La 5*d* contributions emerge above the Fermi level (~4 eV), with ~2–3 electrons/eV at the conduction region. At 50% doping, La 5*d* states broaden and shifts towards +1 to +5 eV, doubling their peak height at ~9 electrons/eV and increasing the DOS near E_F. At 75% doping, La 5*d* states dominate the conduction band (0–10 eV) with more dispersed intensity, suggesting increased delocalisation or hybridisation. Overall, the DOS trends indicate that La doping enhances the DOS near the Fermi level, potentially increasing carrier concentration and influencing electron–phonon coupling in MgB_2.

Table 3. Electronic band structure of pure and La-doped 2×2×2 supercell MgB_2

Dopant & concentration	Band Structure	Band Gap (eV)
Pure MgB_2	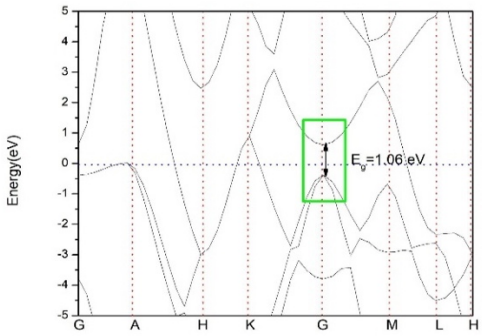	1.06 (indirect)
La-25%	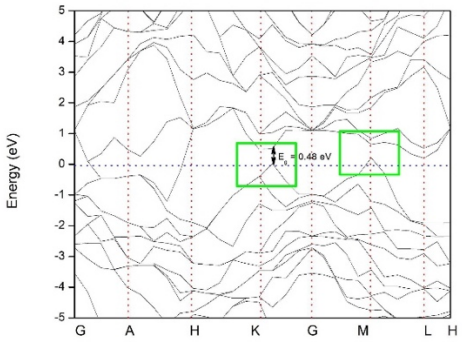	0.48 (indirect)
La-50%	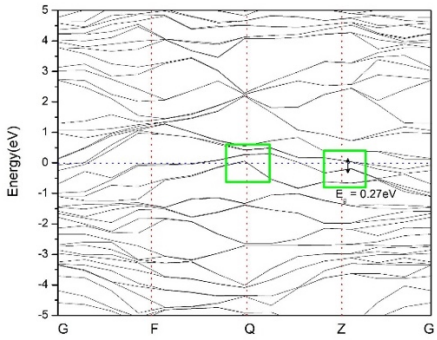	0.27 (indirect)
La-75%	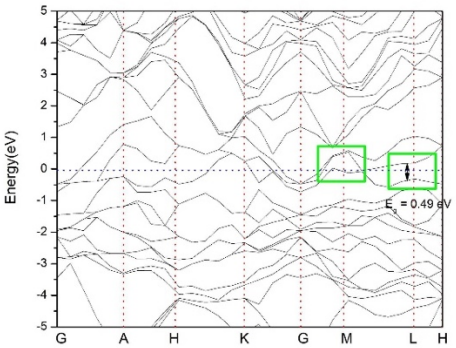	0.49 (indirect)

Table 4. Density of States (DOS) of pure and La-doped 2×2×2 supercell MgB_2

Dopant & concentration	Merged DOS Graph	Dominant Orbitals
Pure MgB_2	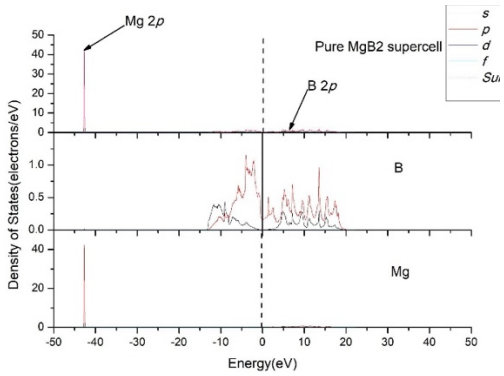	Valence band, V_B = Mg 2*p* Conduction band, V_C = B 2*p*
La-25%	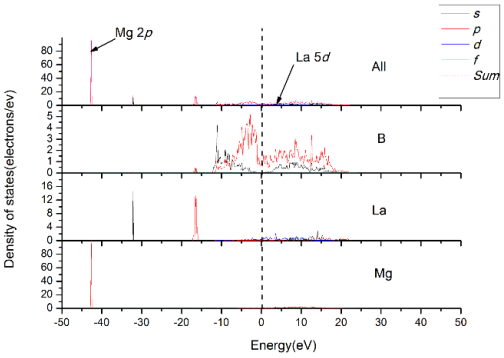	Valence band, V_B = Mg 2*p* Conduction band, V_C = La 5*d*
La-50%	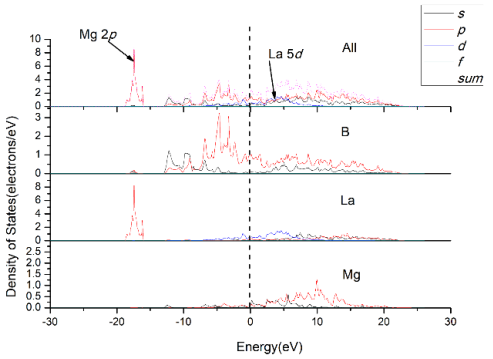	Valence band, V_B = Mg 2*p* Conduction band, V_C = La 5*d*
La-75%	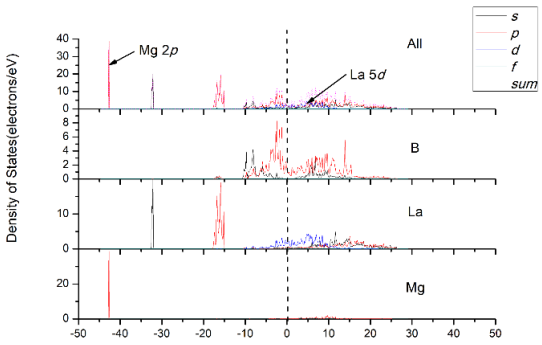	Valence band, V_B = Mg 2*p* Conduction band, V_C = La 5*d*

CONCLUSIONS

Structural analysis shows that La doping induces lattice expansion, particularly along the *a* and *c* axes, with distortions are most significant at 75% doping. The La–B bond lengths exceeded the original Mg–B bond lengths, reflecting strain from the larger ionic radius of La. Electronically, all La-doped structures retained an indirect band gap, consistent with the semi metallic character of MgB_2, but exhibited reduced band gaps, most notably at 50% doping (0.27 eV). DOS analysis showed that La 5*d* orbitals dominate the conduction band, while Mg 2*p* and B 2*p* contribute to the valence band. These results demonstrate that La substitution effectively modifies the structural and electronic properties of MgB_2, potentially enhancing its superconducting behaviour.

ACKNOWLEDGMENTS

The authors gratefully acknowledge the facilities and support provided by the Ionic Materials & Devices (iMADE) Research Laboratory, Institute of Science, Universiti Teknologi MARA (UiTM).

REFERENCES

1. Sheahen TP. *Introduction to High-Temperature Superconductivity*. NY: Kluwer Academic Publishers, 2002.
2. Matsuno S, Ushio H, Suwa Y and Kamimura H. Mechanism of superconductivity. *Int. J. Mod. Phys. B*. 1997;11(32);3815–3831.
3. Boeri L. *Understanding Novel Superconductors with Ab Initio Calculations*. NY: Springer, 2018.
4. Nagamatsu J, Nakagawa N, Muranaka T, Zenitani Y and Akimitsu J. Superconductivity at 39 K in magnesium diboride. *Nature*. 2001;410(6824);63-64.
5. Blöchl P E. *Projector augmented-wave method*. *Physical Review B.* 1994;50(24); 17953.
6. Sun YY, Yang GZ and Wang ZY. Effects of La doping on the structural and superconducting properties of MgB_2. *Journal of Alloys and Compounds.* 2010; 493(1–2);140–144.
7. Shahabuddin M, Alzayed NS, Madhar NA, Qaid SA and Ramay M. Impact of carbon-based doping on the structural and superconducting properties of MgB_2: A comparative study. *Journal of Superconductivity and Novel Magnetism*. 2025;38(2);102.
8. Jiang Y and Liang Y. Comparison of electronic structures, thermodynamic, optical and mechanical properties of MgB_2 and $MgMB_4$ (M= Al, Pb, W) based on first-principles. *Materials Today Communications*. 2024;40;110055.
9. Singh PP. Role of boron p-electrons and holes in superconducting MgB_2, and other diborides: a fully relaxed, full-potential electronic structure study. *Physical Review Letters*. (2001);87(8);087004.
10. Medvedeva NI, Ivanovskii AAL, Medvedeva JE and Freeman AJ. Electronic structure of superconducting MgB_2 and related binary and ternary borides. *Physical Review B*. 2001;64(2);020502.

11. Cheng CH, Zhao Y, Zhu XT, Nowotny J, Sorrell C, Finlayson T and Zhang H. Chemical doping effect on the crystal structure and superconductivity of MgB_2. *Physica C.* 2003;386;588-592.
12. Kimishima Y, Uehara M, Kuramoto T, Takano S. and Takami S. La-doping effects on pinning properties of MgB_2. *Physica C*. 2004;412; 402-406.
13. Shekhar C, Giri R, Tiwari RS, Rana DS, Malik SK and Srivastava ON. Effect of La doping on microstructure and critical current density of MgB_2. *Superconductor Science and Technology*. 2005;18(9);1210-1215.
14. Clark SJ, Segall MD, Pickard CJ, Hasnip PJ, Probert MI, Refson K and Payne MC. First principles methods using CASTEP. *Zeitschrift für kristallographie-crystalline materials*. 2005;220(5-6);567-570.
15. Shi L, Gu Y, Qian T, Li X, Chen L, Yang Z, Ma J and Qian Y. Synthesis of ultrafine superconducting MgB_2 by a convenient solid-state reaction route. *Physica C.* 2004;405(3-4);271–274.
16. Ceperley DM and Alder BJ. Ground state of the electron gas by a stochastic method. *Physical Review Letters*. 1980;45(7);566.
17. Perdew JP, Burke K and Ernzerhof M. Generalised gradient approximation made simple. *Physical Review Letters*. 1996;77(18);3865.
18. Perdew JP, Ruzsinszky A, Csonka GI, Vydrov OA, Scuseria GE, Constantin LA, Zhou X and Burke K. Restoring the density-gradient expansion for exchange in solids and surfaces. *Physical Review Letters*. 2008;100(13);136406.
19. Kuganathan N, Dornheim M, Grant DM and Ling SA density functional theory study of defective and doped structures of MgB_2 and their interaction with hydrogen. *Materials Chemistry and Physics*. 2024;324;129677.
20. Jiang Y and Liang Y. Enhancing mechanical properties of MgB_2 superconductors through Nb substitution: a first-principles study. *Physica B: Condensed Matter*. 2024;683;415931.
21. Van de Walle CG and Neugebauer J. First-principles calculations for defects and impurities: Applications to III-nitrides. *Journal of Applied Physics*, 2004;95(8);3851-3879.
22. Segall MD, Lindan PJ, Probert MA, Pickard CJ, Hasnip PJ, Clark SJ and Payne MC. First-principles simulation: ideas, illustrations and the CASTEP code. *Journal of Physics: Condensed Matter*. 2002;14(11);2717.
23. Kortus J, Mazin II, Belashchenko KD, Antropov VP and Boyer, LL. Superconductivity of metallic boron in MgB_2. *Physical Review Letters*. 2001;86(20); 4656.